Supporting Information

mFES: A robust *m*olecular *F*inite *E*lement *S*olver for electrostatic energy computations

*I Sakalli†, J Schöberl‡, EW Knapp†**

†Freie Universität Berlin, Institute of Chemistry and Biochemistry, Fabeckstr. 36a, Berlin 14195, Germany

‡Technische Universität Wien, Institute for Analysis and Scientific Computing, Wiedner Hauptstraße 8–10, Vienna 1040, Austria

Table of contents

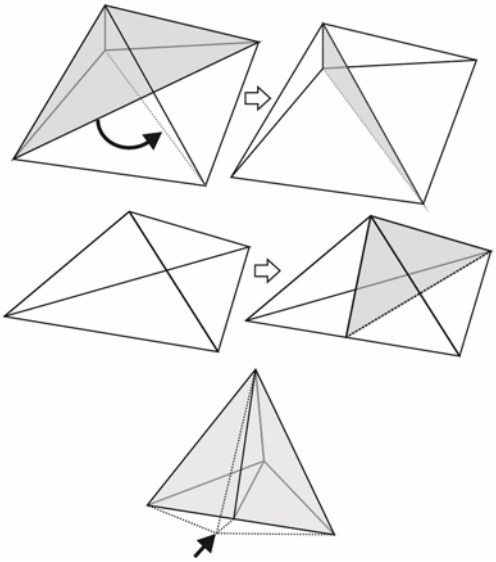

Figure S1. Optimization of tetrahedrons with NETGEN[1]. **top**: tetrahedron face swap: The separating wall between two adjacent tetrahedrons is swapped, which requires that one triangle from each tetrahedron must be in the same plane. If two triangles are only nearly in the same plane, the corresponding nodes are shifted slightly to establish planarity before applying the face swap. **middle**: tetrahedron split: A tetrahedron with a long edge is split in two by a plane which cuts the long edge and contains the two nodes opposite to this edge. **bottom**: tetrahedron collapse: If two triangles have a short common edge, the tetrahedrons built on top of such slim triangles can collapse to triangles by merging the two corner points of the short common edge. As a result one grid point and two tetrahedrons are eliminated.

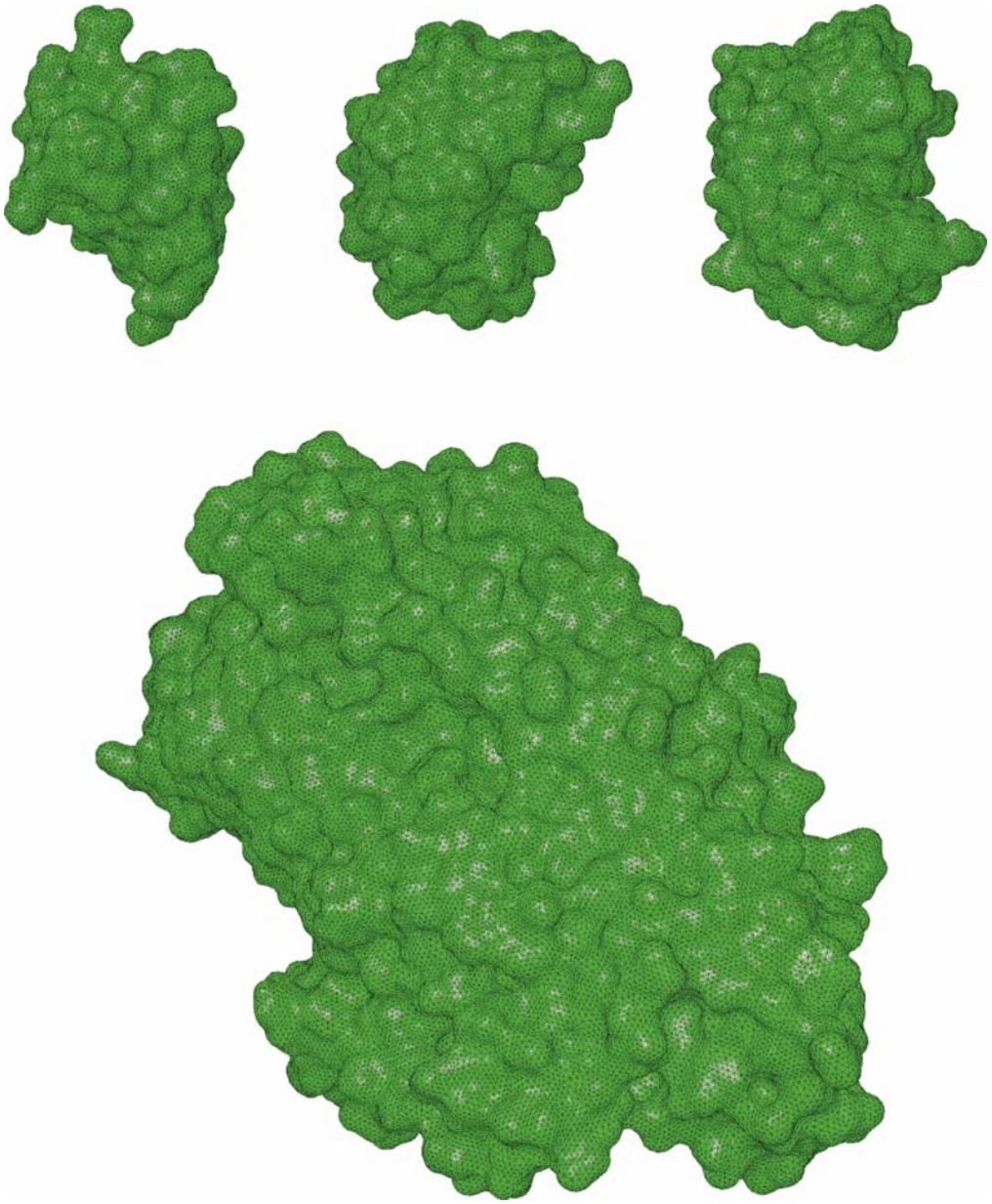

Figure S2. Four proteins used for the computation of solvation energies. **top, left to right**: bovine pancreatic trypsin inhibitor[2] (bpti), barnase[3], lysozyme [4]. **bottom**: cytochrome c oxidase[5].

Table S1. NIST constants and expressions used in calculations

expression / constant	values	units
$\boldsymbol{\varepsilon_0}$	8.85418782×10^{-12}	$\frac{s^4\cdot A^2}{m^3\cdot kg}$
$\mathbf{e_0}$	$1.60217656\times 10^{-19}$	C
$\mathbf{N_A}$	6.0221415×10^{23}	mol^{-1}
ΔG_{Born}	-164.98586	$\frac{z^2}{r}\cdot\frac{kJ}{mol}$
$\boldsymbol{\kappa^2}$	8.43249149	$\frac{I}{\varepsilon_r}\cdot\frac{1}{\AA^2}$

Table S2. ΔG_{Born} electrostatic solvation energy of a unit charge in center of sphere of radius $r_{Born} = 3$ Å, $\varepsilon_{in} = 4$, $\varepsilon_{out} = 80$. Comparison of APBS and mFES solver with varying ionic strength I, listing the numerical values for Fig. (8) in main text.

I [mol/l]	APBS fine[a,b]	APBS coarse[a,c]	mFES[d]	analytical result
0.01	-40.6542	-40.9927	-40.7276	-40.6188
0.02	-37.7509	-38.0969	-37.8258	-37.7153
0.05	-33.9976	-34.3215	-34.0675	-33.9565
0.1	-31.4309	-31.7182	-31.4927	-31.3823
0.15	-30.0910	-30.3521	-30.1470	-30.0374
0.2	-29.2216	-29.4631	-29.2734	-29.1643

[a] The point density at the atomic vdW spheres is set to 10 points/Å^2, which is the recommended value in APBS.
[b] $n^3 = 193^3 = 7.2\ 10^6$ grid points with 0.05 Å lattice constant
[c] $n^3 = 65^3 = 2.7\ 10^5$ grid points with 0.25 Å lattice constant
[d] Second order approximation is used corresponding to an average distance between neighbor grid points of 0.175 Å inside the Born ion sphere resulting in a total of 34,335 grid points, which is 1/8 of the number grid points used for the coarse resolution with FD. The spherical asymptotic boundary surface is at a distance of 10^5 Å from the center.

CPU time ratio of solving linear equation systems

Solving the linear equation system is the computationally most expensive part in FD methods. Hence, CPU times for solving the linear equations for four different proteins are shown as a ratio between APBS and mFES (Fig. S5). Here, CPU times for preparing the linear equation system like generating the tetrahedral grid of the molecular model are not included. mFES reduces the CPU time to solve the linear equation system by at least one order of magnitude because the number of equations is significantly smaller with the FE method. mFES uses the linear equation solver MUMPS (*M*ultifrontal *M*assively *P*arallel sparse direct *S*olver).[6-8]

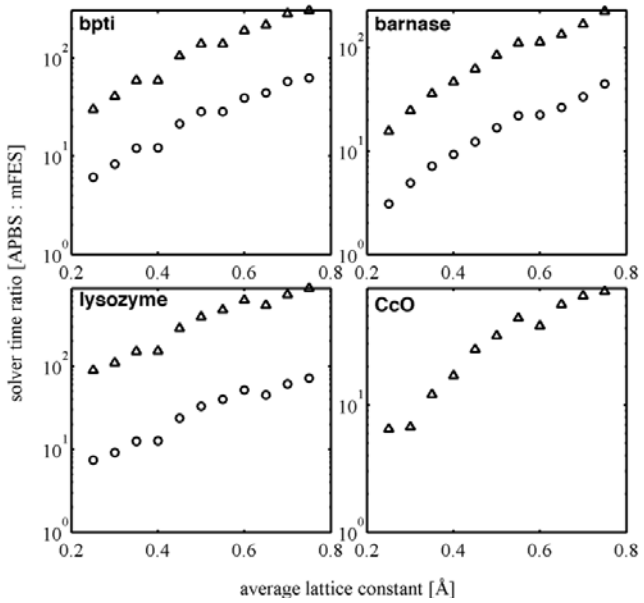

Figure S3. CPU time ratios solving linear equation systems for four proteins. Solver time ratio of APBS fine to mFES (△) and APBS coarse to mFES (○) are plotted versus the average edge length h_S on the molecular surface using mFES. Calculations are done with two APBS models (fine and coarse) for every molecule and one model for each average surface edge length generated with mFES. The ratio between APBS to mFES is increasing from lower to higher lattice constant because the molecular models computed by mFES are getting coarser without losing much accuracy in electrostatic calculations compared to FD method.

References.

(1) Schöberl, J. NETGEN An Advancing Front 2D/3D-Mesh Generator Based on Abstract Rules. *Comput. Vis. Sci.* **1997**, *1*, 41–52.

(2) Berndt, K. D.; Güntert, P.; Orbons, L. P.; Wüthrich, K. Determination of a High-Quality Nuclear Magnetic Resonance Solution Structure of the Bovine Pancreatic Trypsin Inhibitor and Comparison with Three Crystal Structures. *J. Mol. Biol.* **1992**, *227*, 757–775.

(3) Martin, C.; Richard, V.; Salem, M.; Hartley, R.; Mauguen, Y. Refinement and Structural Analysis of Barnase at 1.5 A Resolution. *Acta Crystallogr. D. Biol. Crystallogr.* **1999**, *55*, 386–398.

(4) Ramanadham, M.; Sieker, L. C.; Jensen, L. H. Refinement of Triclinic Lysozyme: II. The Method of Stereochemically Restrained Least Squares. *Acta Crystallogr. B.* **1990**, *46 (Pt 1)*, 63–69.

(5) Svensson-Ek, M.; Abramson, J.; Larsson, G.; Törnroth, S.; Brzezinski, P.; Iwata, S. The X-Ray Crystal Structures of Wild-Type and EQ(I-286) Mutant Cytochrome c Oxidases from Rhodobacter Sphaeroides. *J. Mol. Biol.* **2002**, *321*, 329–339.

(6) Amestoy, P. R.; Davis, T. A.; Duff, I. S. An Approximate Minimum Degree Ordering Algorithm. *SIAM J. Matrix Anal. Appl.* **1996**, *17*, 886–905.

(7) Amestoy, P. R.; Duff, I.; L'Excellent, J. Y. MUMPS MUltifrontal Massively Parallel Solver. *Tech. Report, TR/PA/98/02* **1998**.

(8) Amestoy, P. R.; Duff, I. S.; L'Excellent, J.-Y. Multifrontal Parallel Distributed Symmetric and Unsymmetric Solvers. *Comput. Methods Appl. Mech. Eng.* **2000**, *184*, 501–520.